

Modeling the mass balance and fate of copper in San Diego Bay

D. B. Chadwick, A. Zirino, I. Rivera-Duarte, C. N. Katz, and A. C. Blake

Environmental Sciences Division, Code 2362, SPAWAR Systems Center San Diego, 53560 Hull Street, San Diego, California 92152-5001

Abstract

Because of its presence in antifouling coatings, stormwater, and industrial and municipal discharges, copper is a ubiquitous contaminant in estuarine and coastal environments. We integrated a system-wide field program with a one-dimensional model to evaluate the overall mass balance of copper in a representative coastal harbor, San Diego Bay, California. Field results from four surveys over 1 yr showed remarkably similar distributions of total copper, with a general increase from the ocean into the Bay followed by a slight decrease in the inner Bay. Total copper concentrations ranged from 5 nmol L⁻¹ to nearly 60 nmol L⁻¹. Highest levels for both total and dissolved copper were observed during the winter. Results from a one-dimensional model accounting for the balance of sources, flushing, and losses to the sediment illustrated the importance of accounting for losses of copper to the sediment, without which water column concentrations are overestimated by as much as a factor of five. The time scale for the loss term is on the order of 8–10 d. The model reproduced the field measurements quite well with a loss term controlled by partitioning and settling parameters. The overall balance of total copper in the Bay appears to be split between losses to the ocean via tidal flushing and losses to the sediments via settling. Settling plays an important role in the fate of copper in the Bay, and the sediments are a key endpoint for copper.

Because of its broad use in antifouling coatings, copper is one of the most ubiquitous and problematic contaminants in harbor, estuarine, and coastal marine environments (Moffett et al. 1997; Terlizzi et al. 2001; Ranke 2002). Other general sources of copper include municipal discharges, industrial discharges, stormwater and nonpoint source (NPS) runoff, sediment fluxes, and mining and ore handling (Nriagu 1996; Rivera-Duarte and Flegal 1997; Eriksen et al. 2001). Previous studies in San Diego Bay suggest that the combination of these loadings has led to chronic elevations of copper in ambient water at levels that approach or exceed the water quality criteria in some areas (Flegal and Sañudo-Wilhelmy 1993; Zirino et al. 1998a; Esser and Volpe 2002). Subsequent transport of this copper to the sediments also presents a pathway for fate and the potential for ecological impairment (Fairey et al. 1998). Although there is still considerable debate as to the site-specific toxicity of copper in marine waters and sediments, there is clearly a need to understand the overall loading, distribution, and fate of copper in urbanized coastal harbors and bays such as San Diego Bay.

The range of previous efforts to measure and model the transport, fate, and speciation of copper reflect the breadth and complexity of the problem (Klinkhammer and Bender 1981; Santschi et al. 1984; Rozan and Benoit 2001). The majority of these efforts have relied on the assumption of equilibrium between various copper species and estimated or modeled stability constants (Tipping 1994; Di Toro et al. 2001). Wood et al. (1995) demonstrated the potential im-

portance of considering interspecies kinetics in modeling copper fate in South San Francisco Bay. Their diagnostic model showed that the kinetics of aqueous speciation and adsorption could account for a significant fraction of the basin-scale variability in partitioning. Wood et al. (1995) and Rozan and Benoit (2001) also pointed out many of the shortfalls of existing models, including the absence of adequate source data, overall loss rates to the sediment, the uncertainty in rate and equilibrium constants, the weak relation between bulk measures of organic matter and complexation capacity, and the potential temporal and spatial variability of various binding matrices.

In general, the distribution of copper in the water column of a bay is controlled by a balance between sources, transport to the sediments (sinks), and exchange with the ocean (flushing). Thus our ability to understand the balance of copper in a coastal harbor such as San Diego Bay depends on the effectiveness with which we can either measure or model these processes on a system-wide scale. San Diego Bay is ideally suited for this purpose because the sources of copper are relatively well characterized (Johnson et al. 1998; Valkirs et al. 2003), the sources are chronic in nature, resulting in near-steady-state conditions (Flegal and Sañudo-Wilhelmy 1993), and previous studies of the tidal exchange and salinity balance provide an independent means of verifying the flushing properties of the Bay (Largier et al. 1996; Chadwick and Largier 2000).

In this article, we combine a calibrated, one-dimensional exchange model of San Diego Bay with a scale-matched set of field measurements to evaluate the overall mass balance of copper and to constrain the rate constants of transformation and fate processes for copper throughout the Bay.

Methods

Field program—Four field surveys were performed in San Diego Bay during the period from August 2000 through September 2001 (Table 1). The surveys were designed specifi-

Acknowledgments

The authors acknowledge the assistance of Joel Guerrero and Lora Kear for analytical support, Jon Groves and Brad Davidson for field support, P. F. Wang for critical analysis of the modeling work, and Chip Johnson and Aldis Valkirs for assistance with the source analysis. The manuscript was significantly improved by comments received from two anonymous reviewers.

This study was supported by the Office of Naval Research 6.2 program contract N6601-97-D-5028 and from the Strategic Environmental Research and Development Program under project CP-1156.

Table 1. Field surveys in San Diego Bay.

Survey	Date	Start time (local time, h)	End time (local time, h)	Low tides (local time, h)	High tides (local time, h)
SD26	30 Aug 2000	0830	1900	0446, 1647	1101, 2253
SD27	30 Jan 2001	0800	1700	0639, 1845	1214
SD31	11 May 2001	0730	1600	0704, 1750	1356
SD32	19 Sep 2001	0800	1800	0507, 1740	1120, 2348

cally to provide distribution data for salinity and copper for calibration and evaluation of the model. All surveys were performed using the Navy's Marine Environmental Survey Capability (MESC) installed aboard the 12-m research vessel RV *Ecos*. Each survey consisted of a transect from the mouth of the Bay to the head (Fig. 1). The transect layout included two transverse legs within each of 27 predefined sampling boxes (including two side basins). The sampling boxes had an axial length scale of about 1 km to correspond with the layout of the one-dimensional model.

Underway measurements and sampling—During a transect, continuous measurements and composite samples were collected with the MESC real-time system with the use of both a towed sensor package and a trace metal clean Teflon® seawater flow-through system. Sensors in the towed package included a conductivity, temperature, and depth (CTD) profiler outfitted with pH and dissolved oxygen sensors, a light transmissometer, and an ultraviolet (UV) fluorometer for hydrocarbon detection. The onboard sensors included two fluorometers (UV and chlorophyll), two automated trace metal analyzers (TMAs) for copper measurement, an acoustic Doppler current profiler (ADCP), a digital fathometer, and a differential global positioning system (DGPS) navigation re-

ceiver. The TMA is an automated Au-film potentiometric stripping analysis method for determining dissolved metals (Zirino et al. 1998b). Continuous data were typically collected while moving at speeds up to 11 km h⁻¹. At a 4-Hz sampling rate, the along-track spatial resolution of the data was less than 1 m. The vessel was stopped to perform vertical profiles for every other box segment; otherwise, all sampling was performed at a depth of about 2 m. The composite samples were collected from each of the box regions shown in Fig. 1 by continuously pumping into precleaned, 20-liter carboys. Subsamples taken from the composite samples were analyzed for total and dissolved copper, copper complexation capacity, dissolved organic carbon (DOC), and total suspended sediments (TSS).

Copper analysis—Total and dissolved copper concentrations in composite samples were determined by clean techniques following the method of Bruland et al. (1985). Subsamples were drawn from the 20-liter composite samples with a Teflon pumping system on the bow of the RV *Ecos*. Total copper samples were collected unfiltered, and dissolved copper samples were filtered onboard with 0.45- μ m all-polypropylene Calix cartridge filters. The samples were acidified to pH ≤ 2 with Ultrex-grade nitric acid in a class 100 all-polypropylene clean station. Copper in the samples was preconcentrated by liquid-liquid extraction with ammonium pyrrolidinedithiocarbamate and diethylammonium diethyldithiocarbamate and was measured by graphite furnace atomic spectrometry using stabilized temperature platforms and the method of standard additions. The efficiency of the extraction was $102 \pm 8.6\%$ (average \pm SD, $n = 4$) for the National Institute of Standards and Technology standard reference material 1643d and $98 \pm 8.8\%$ ($n = 18$) for Canadian Research Council coastal seawater standards CASS3 and CASS4. The variation of replicate analysis was $\leq 12\%$, and the method limit of detection was $0.004 \pm 0.002 \mu\text{g L}^{-1}$ ($n = 8$).

TSS and DOC analysis—Subsamples from the composites collected for TSS were analyzed by filtering approximately 900 ml through predried and preweighed glass fiber filters (1.2 μ m nominal pore size). The filters were rinsed with deionized water to remove dissolved salts then dried and weighed to determine the mass of the filtered solids. For DOC, water from each composite sample was filtered through 0.7- μ m nominal pore size precombusted glass fiber filters into 5-ml amber ampoules containing 8 μ l H₂PO₄. The ampoules were heat sealed and stored frozen until DOC analysis. Milli-Q® blanks and method blanks (rinsed through

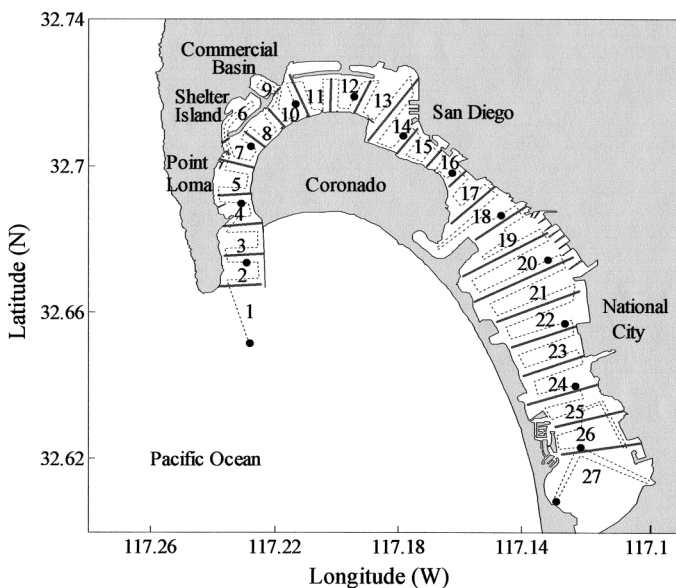


Fig. 1. Map of San Diego Bay showing model/sampling segments (solid lines with numbers), survey transect (dashed line), and vertical profile locations (solid circles).

syringe and filter unit) were conducted at the beginning, middle, and end of each sampling event. Blanks were generally low ($<25 \mu\text{mol L}^{-1}$) but were as high as $35 \mu\text{mol L}^{-1}$. DOC was measured with an MQ1001 high-temperature combustion total organic carbon analyzer (Qian and Mopper 1996). Sodium phthalate was used to make standards that were run for each 30 samples. Standard curves for all DOC analyses had correlation coefficients >0.98 .

Tidal normalization—Data from the onboard sensors were binned and averaged within each of the box regions. The time to complete a survey generally spanned about 8–10 h (Table 1). This meant that considerable changes in the tidal condition occurred during each survey, and these tidal conditions were not always the same for each survey. To account for this, all of the box-averaged data, along with the data from the composite samples, were corrected for tidal advection to an average tidal condition. This was done by first displacing each sample location by the corresponding tidal excursion at that location. The data were then spatially interpolated back onto the original 25-box grid.

Model description—The one-dimensional, steady-state box model SD-1D provided an initial assessment of the copper balance in San Diego Bay and estimates of copper loss rates to the sediment. This model gives a one-dimensional, steady-state solution to the balance of conservative and non-conservative constituents. It has the advantage of rapid formulation and run times relative to more sophisticated numerical models but lacks the ability to simulate time-varying concentrations and has relatively coarse spatial resolution.

San Diego Bay is a seasonally hypersaline embayment (Largier et al. 1996, 1997). Exchange between the Bay and the ocean is controlled by tidal pumping via a single, relatively narrow entrance channel (Chadwick and Largier 2000). Infrequent fresh water inflow, combined with a warm climate and consistent westerly wind patterns, leads to a net evaporation of water from the Bay, which in turn causes the Bay to become hypersaline. The salt balance is therefore determined by the balance between the increase in salinity because of evaporation and the decrease in salinity because of tidal exchange with the ocean. This balance tends to reach a quasi-steady state by July and persists until the first significant winter rains in November or December (Largier et al. 1997). These characteristics, along with its relatively one-dimensional morphology (long and narrow), make San Diego Bay ideally suited to models such as SD-1D.

The model SD-1D solves the discrete, tidally averaged, steady-state mass balance equation for each defined segment of San Diego Bay following the general form

$$A_x u c|_i - A_x u c|_{i+1} = \frac{A_x D}{l} \left| (c_j - c_{j-1}) - \frac{A_x D}{l} \right|_{i+1} (c_{j+1} - c_j) + S_j - L_j \quad (1)$$

where A_x is the cross-sectional area, u is the tidally averaged advection, c is the concentration of the species of interest (e.g., salt, copper), D is the tidal dispersion coefficient, l is the longitudinal distance between segments, S is the source term, L is a configurable loss term, and the subscript i refers

to the mouthward boundary of the j th box. The model was segmented into a series of 25 boxes along the axis of the Bay (Fig. 1), resulting in a spatial resolution of about 1 km. Two side-basin boxes (Shelter Island [6] and Commercial Basin [9]) also were designated for sampling purposes but were not evaluated in the model.

The model was tuned using the salinity balance for the Bay. Assuming precipitation and river flows to be negligible and evaporation to be dominant, we have $S = L = 0$, and

$$u = \frac{e \sum_{j+1}^{25} A_x}{A_x} \quad (2)$$

where e is the evaporation rate, and A_x is the box surface area. The evaporation rate was estimated at 0.43 cm d^{-1} on the basis of long-term evaporation rates reported for San Diego Bay (Largier et al. 1997). The volume, surface, and cross-sectional areas of each box were developed from detailed bathymetric data for San Diego Bay (Wang et al. 1998).

Copper loadings to each box were determined on the basis of the estimates of Johnson et al. (1998), which were updated to account for recent improvements in estimates for various input rates and to incorporate estimates for particulate copper (Table 2; Fig. 2). Johnson et al. (1998) compiled source estimates for copper releases from civilian, commercial, and Navy hull coating leachate; civilian and Navy hull cleaning; other ship discharges (e.g., cooling water); point source discharges; stormwater runoff; and atmospheric deposition.

Source estimates for Navy, civilian, and commercial hull coating leachate to each box region were calculated as

$$S_{\text{leach}} = \sum_{\text{classes}} \left(r_{\text{leach}} \sum_{\text{ships}} f_{\text{port}} A_{\text{wet}} \right) \quad (3)$$

where A_{wet} is the wetted surface area of the vessel class (Navy, civilian, commercial), f_{port} is the fraction of time the ship is in port, and r_{leach} is the average copper leach rate for the class. Wetted areas for Navy ships in each box region were summed on the basis of reported individual hull areas (Johnson et al. 1998). The total wetted area for Navy ships in the entire Bay was estimated at $\sim 309 \times 10^3 \text{ m}^2$. Wetted area for civilian and commercial hulls were based on those reported by Johnson et al. (1998), with total areas of $282 \times 10^3 \text{ m}^2$ and $2,807 \times 10^3 \text{ m}^2$, respectively. The fraction of time in port was estimated for individual Navy ships and subclasses of commercial ships (e.g., cruise ships, cargo ships, tugs) on the basis of the values reported by Johnson et al. (1998). The overall average of time in port for Navy ships was $\sim 48\%$, whereas for commercial ships, the overall average was $<2\%$. For civilian pleasure boats, the fraction of time in port was taken as 100%. Copper leach rates were updated from Johnson et al. (1998) as $3.9 \mu\text{g cm}^{-2} \text{ d}^{-1}$ for Navy ships and $8.1 \mu\text{g cm}^{-2} \text{ d}^{-1}$ for pleasure boats on the basis of the recent compilation of measurements from Valkirs et al. (2003).

Table 2. Summary of copper sources (kg yr⁻¹) to San Diego Bay. See footnotes and text for description of and references for the development of source terms.

Box	Cubic fraction	Nonpoint source				Antifouling paint sources					Other sources†		Totals	
		Wet weather		Dry weather		Navy hull leach¶	Navy hull clean#	Civilian hull leach¶	Civilian hull clean**	C o m - mer- cial vessel leach¶	Navy other	Point source	Dry weather	Wet weather
		Direct rain-fall‡	Storm-water§	Base-flow†	Atmos-pheric loading									
1	d	0	0	0	0	0	0	0	0	0	0	0	0	0
	p	0	0	0	0	0	0	0	0	0	0	0	0	0
	t	0	0	0	0	0	0	0	0	0	0	0	0	0
2	d	0	0	0	0	0	0	0	0	0	0	0	0	0
	p	0.5	0	0	1.2	0	0	0	0	0	0	0	1.2	1.7
	t	0.5	0	0	1.2	0	0	0	0	0	0	0	1.2	1.7
3	d	0	0	0	0	0	0	0	0	0	0	0	0	0
	p	0.4	0	0	1.1	0	0	0	0	0	0	0	1.1	1.5
	t	0.4	0	0	1.1	0	0	0	0	0	0	0	1.1	1.5
4	d	0	42	0.9	0	257	8	0	0	0	433	0	699	741
	p	0.4	10	0.2	1.1	0	139	0	0	0	0	0	140	150
	t	0.4	51	1.1	1.1	257	147	0	0	0	433	0	839	891
5	d	0	42	0.9	0	0	0	0	0	0	0	0	0.9	42
	p	0.4	10	0.2	1.0	0	0	0	0	0	0	0	1.2	11
	t	0.4	51	1.1	1.0	0	0	0	0	0	0	0	2.1	54
7	d	0	42	0.9	0	6	0	2,133	43	0	0	0	2,183	2,225
	p	0.7	10	0.2	1.8	0	0	0	746	0	0	0	748	758
	t	0.7	51	1.1	1.8	6	0	2,133	789	0	0	0	2,931	2,983
8	d	0	42	0.9	0	0	0	0	0	0	0	0	0.9	42
	p	0.3	10	0.2	0.7	0	0	0	0	0	0	0	0.9	11
	t	0.3	51	1.1	0.7	0	0	0	0	0	0	0	1.8	53
10	d	0	42	0.9	0	6	0	699	14	0	0	0	720	761
	p	0.6	10	0.2	1.4	0	0	0	244	0	0	539	785	795
	t	0.6	51	1.1	1.4	6	0	699	258	0	0	539	1,505	1,557
11	d	0	42	0.9	0	0	0	1,551	31	0	0	0	1,583	1,625
	p	0.8	10	0.2	2.1	0	0	0	542	0	0	0	544	555
	t	0.8	51	1.1	2.1	0	0	1,551	574	0	0	0	2,128	2,180
12	d	0	42	0.9	0	0	0	0	0	0	0	0	0.9	42
	p	0.4	10	0.2	1.0	0	0	0	0	0	0	0	1.2	11
	t	0.4	51	1.1	1.0	0	0	0	0	0	0	0	2.1	54
13	d	0	42	0.9	0	113	0	693	14	0	303	0	1,124	1,166
	p	0.7	10	0.2	1.9	0	0	0	242	0	0	0	244	255
	t	0.7	51	1.1	1.9	113	0	693	256	0	303	0	1,368	1,420
14	d	0	42	0.9	0	113	0	466	9	49	303	0	941	983
	p	0.6	10	0.2	1.6	0	0	0	163	0	0	0	165	175
	t	0.6	51	1.1	1.6	113	0	466	172	49	303	0	1,106	1,158
15	d	0	8	0.9	0	0	0	0	0	0	0	0	0.9	9.2
	p	0.3	2	0.2	0.9	0	0	0	0	0	0	0	1.1	3.4
	t	0.3	10	1.1	0.9	0	0	0	0	0	0	0	1.9	13
16	d	0	8	0.9	0	0	0	0	0	76	0	0	77	85
	p	0.3	2	0.2	0.7	0	0	0	0	0	0	0	0.9	3.1
	t	0.3	10	1.1	0.7	0	0	0	0	76	0	0	78	88
17	d	0	2	0.9	0	0	0	66	1	76	0	0	145	147
	p	0.5	1	0.2	1.2	0	0	0	23	0	0	0	25	26
	t	0.5	3	1.1	1.2	0	0	66	25	76	0	0	169	172
18	d	0	2	0.9	0	38	0	342	7	0	5	0	392	394
	p	0.8	1	0.2	2.0	0	0	0	119	0	0	837	959	960
	t	0.8	3	1.1	2.0	38	0	342	126	0	5	837	1,351	1,355
19	d	0	382	0.5	0	649	7	0	0	3	794	0	1,455	1,837
	p	0.9	89	0.1	2.3	0	124	0	0	0	0	359	485	575
	t	0.9	471	0.6	2.3	649	131	0	0	3	794	359	1,940	2,412
20	d	0	0	0.5	0	611	7	0	0	0	790	0	1,409	1,409
	p	1.2	0	0.1	2.9	0	124	0	0	0	0	0	127	128
	t	1.2	0	0.6	2.9	611	131	0	0	0	790	0	1,535	1,537

Table 2. Continued.

Box	Cubic fraction*	Nonpoint source				Antifouling paint sources					Other sources†		Totals	
		Wet weather		Dry weather		Navy hull leach¶	Navy hull clean#	Civilian hull leach¶	Civilian hull clean**	Commercial vessel leach¶	Navy other	Point source	Dry weather	Wet weather
		Direct rainfall‡	Storm-water§	Base-flow†	Atmospheric loading									
21	d	0	149	0.5	0	611	7	0	0	0	790	0	1,409	1,557
	p	1.1	34	0.1	2.8	0	124	0	0	0	0	0	127	162
	t	1.1	183	0.6	2.8	611	131	0	0	0	790	0	1,535	1,720
22	d	0	0	0.5	0	0	0	399	8	0	0	0	408	408
	p	0.9	0	0.1	2.2	0	0	0	140	0	0	0	142	143
	t	0.9	0	0.6	2.2	0	0	399	148	0	0	0	550	551
23	d	0	16	17.1	0	0	0	0	0	152	0	0	169	185
	p	0.8	4	4.0	1.9	0	0	0	0	0	0	0	5.9	10
	t	0.8	20	21.0	1.9	0	0	0	0	152	0	0	175	196
24	d	0	16	17.1	0	0	0	0	0	0	0	0	17	33
	p	0.8	4	4.0	2.0	0	0	0	0	0	0	0	6.0	11
	t	0.8	20	21.0	2.0	0	0	0	0	0	0	0	23	44
25	d	0	16	17.1	0	0	0	661	13	0	0	0	692	708
	p	0.8	4	4.0	2.1	0	0	0	231	0	0	0	237	242
	t	0.8	20	21.0	2.1	0	0	661	244	0	0	0	929	949
26	d	0	16	17.1	0	0	0	538	11	0	0	0	566	582
	p	0.9	4	4.0	2.2	0	0	0	188	0	0	0	194	199
	t	0.9	20	21.0	2.2	0	0	538	199	0	0	0	760	781
27	d	0	266	42.8	0	0	0	788	16	0	0	0	847	1,113
	p	0.8	62	9.9	2.0	0	0	0	275	0	0	324	611	674
	t	0.8	328	52.7	2.0	0	0	788	291	0	0	324	1,458	1,787
Totals	d	0	1,257	124.5	0.0	2,405	30	8,336	169	356	3,418	0	14,839	16,096
	p	16	292	28.9	39.8	0	510	0	2,914	0	0	2,060	5,552	5,860
	t	16	1,549	153.4	39.8	2,405	539	8,336	3,083	356	3,418	2,060	20,391	21,956

* d, dissolved phase; p, particulate phase; t, total.

† Estimated from Johnson et al. (1998).

‡ Estimated from Eq. 6, P. Stang (pers. comm.), and data from the National Weather Service.

§ Estimated from Johnson et al. (1998) and Chadwick et al. (1999).

|| Estimated from Eq. 5, 1990–1995 Air Pollution Control District data, and P. Stang (pers. comm.).

¶ Estimated from Eq. 3, Johnson et al. (1998), and Valkirs et al. (2003).

Estimated from Eq. 4, Johnson et al. (1998), and USEPA (1999).

** Estimated from Eq. 4, Johnson et al. (1998), and USEPA (1999), and K. Schiff (pers. comm.).

The source loading of dissolved copper from Navy and civilian hull cleaning was calculated as

$$S_{\text{clean}} = \sum_{\text{classes}} \left(r_{\text{clean}} \sum_{\text{ships}} n_{\text{clean}} A_{\text{wet}} \right) \quad (4)$$

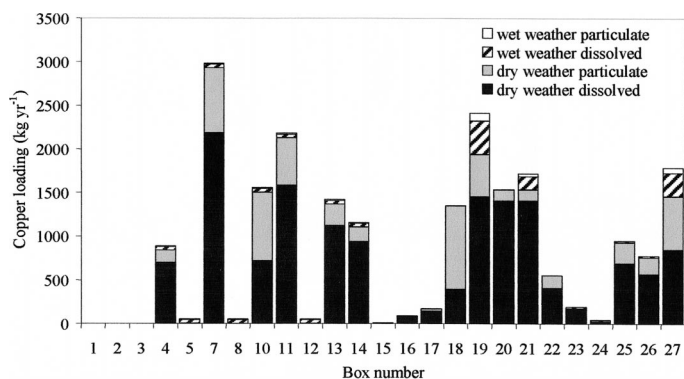


Fig. 2. The estimated copper loading to designated model regions in San Diego Bay.

where n_{clean} is the number of hull cleanings per year, and r_{clean} is the dissolved copper release rate per cleaning. The number of cleanings per year was taken as 0.83 for Navy ships, and 10 for civilian vessels (Johnson et al. 1998). The dissolved copper release rate was estimated at $26 \mu\text{g cm}^{-2} \text{ cleaning}^{-1}$ for Navy ships (USEPA 1999) and $6 \mu\text{g cm}^{-2} \text{ cleaning}^{-1}$ for civilian vessels (K. Schiff pers. comm.). Navy and civilian hull cleaning inputs for particulate copper were calculated from the dissolved estimates by applying the particulate:dissolved ratio reported in USEPA (1999).

Dry weather atmospheric deposition was calculated for each box as

$$S_{\text{atm}} = c_{\text{atm}} v_d A_s \quad (5)$$

where the copper concentration on atmospheric particles (c_{atm}) was taken from the average of 1990–1995 Air Pollution Control District data as 1.0 pmol L^{-1} and the particle deposition velocity (v_d) was taken as 0.5 mm s^{-1} , assuming an average annual wind speed of 3.1 m s^{-1} , a surface roughness factor of 0.02 (smooth sea), and an average particle size

of 2 μm (Stang pers. comm.). Similarly, the input of copper via direct rainfall was estimated as

$$S_{\text{rain}} = c_{\text{rain}} r_{\text{rain}} A_s \quad (6)$$

for each box, where the copper concentration in rain (c_{rain}) was taken to be 25 nmol L^{-1} (Stang pers. comm.), and a rainfall rate (r_{rain}) of 25.1 cm yr^{-1} was used on the basis of data from the National Weather Service.

Stormwater inputs of dissolved copper were updated to use measured event mean concentrations for all available watersheds (Chadwick et al. 1999), with the remaining areas calculated following the simple model method described by Johnson et al. (1998). Particulate copper loading from base-flow and stormwater were calculated with the particulate:dissolved ratio for event mean concentrations.

The results of this analysis indicate total copper loadings of about $20.4 \times 10^3 \text{ kg yr}^{-1}$ and $22 \times 10^3 \text{ kg yr}^{-1}$ for dry weather and wet weather conditions, respectively. Spatially, these sources are fairly evenly distributed throughout the Bay (Fig. 2).

With estimated mixing characteristics, loadings, and ocean boundary condition defined, the total copper balance depends only on the loss rate of copper from the water column to the sediment. Two potential solutions were explored for the loss term. In the first solution, a uniform, first-order loss rate was assumed to apply throughout the Bay such that

$$L_j = k(Vc_i)_j \quad (7)$$

where k is the loss coefficient, V is the box volume, and c_i is the total copper concentration. The loss rate was then adjusted to provide a best fit (least squares) to the measured copper concentrations in the Bay. In the second solution, a simple particle-settling model was applied. This model predicts a loss of copper to the sediment such that

$$L_j = w \left(\frac{Vc_p}{h} \right)_j \quad (8)$$

where c_p is the particulate phase concentration of copper, w is the mean settling rate (assumed to be constant throughout the Bay), and h is the mean depth of the region. A fundamental difference for the settling approach is that it requires knowledge of the particulate copper concentration in order to model the total copper balance. For this purpose, we assumed that a suspended load-dependent equilibrium between the dissolved and particulate phases prevails with a partitioning coefficient defined as

$$K_d = \frac{c_p}{c_d \text{TSS}} \quad (9)$$

where c_d is the dissolved copper concentration, and TSS is the total suspended solids concentration. Because $c_i = c_f + c_d + c_p$, and c_f (the free copper concentration) is generally small (<1%) compared to c_d and c_p , we combine Eqs. 8 and 9 to obtain the loss term of Eq. 10.

$$L_j = wK_d \left\{ \left(\frac{V}{h} \right) \left[\frac{\text{TSS}c_i}{(1 + K_d \text{TSS})} \right] \right\}_j \quad (10)$$

Both of these approaches represent simplifications of the actual sediment-water exchange of copper, which results from a number of specific processes, including particle set-

ling and resuspension, as well as porewater advection and diffusion (Rivera-Duarte and Flegal 1997; Cantwell et al. 2002; Spinelli et al. 2002). However, given the available data, it is not possible to delineate these individual processes. The two approaches provide some initial insight into the overall rate, time scale, and mass transport to the sediment and a net settling velocity that might reflect the combined effect of all sediment exchange processes. The potential contributions of porewater migration mechanisms, although not directly incorporated in the model, are evaluated on the basis of a limited set of field measurements available in the Bay.

For total copper, the model solves the mass balance equation by iteratively marching from the ocean boundary to the head of the Bay and adjusting concentrations until a steady-state mass balance is achieved (zero mass transport through the last box boundary). This steady-state solution, which is based on calibration to measured salinity distributions, has been employed successfully in a broad range of estuarine settings (Dyer 1974; Fischer et al. 1979).

Results

Field results—The salinity distribution during August 2000 (Fig. 3) is typical of the hypersaline conditions that persist in San Diego Bay through much of the summer and fall (Largier et al. 1996). Salinity increases gradually from the mouth toward the head of the Bay, with the strongest gradient near the head. The salinity data were averaged onto the model grid and corrected for tidal advection, and the salinity gradient was calculated along the longitudinal axis of the Bay (Fig. 4). The tidal dispersion coefficients for each segment (D) were then estimated from Eq. 1 on the basis of the best fit to measured salinity distributions during periods of low freshwater during the August and September 2001 cruises and of a previous survey in August 1997 (Katz 1998).

The longitudinal salinity distributions are comparable for the three surveys, resulting in estimated dispersion coefficients ranging from a maximum of about 200 $\text{m}^2 \text{s}^{-1}$ at the mouth to near zero at the head (Fig. 2), consistent with previously published values for coastal bays and estuaries (Fischer et al. 1979). On the basis of these mixing rates, Bay residence times were calculated for local box regions, as well as flushing times for exchange between each box region and the ocean boundary (Fig. 4). Residence times for local box regions ranged from <1 d to ~4 d, with the longest residence times for boxes near the head of the Bay. Flushing times ranged from a few days near the mouth to almost 40 d near the head (Fig. 4).

TMA results from August 2000 provide a representative snapshot of the spatial distribution of copper in San Diego Bay that is based on >60 individual samples (Fig. 3). The contour map developed from these data reveals a general gradient through the Bay, increasing from the mouth to the mid-south Bay, and then decreasing slightly toward the head. Copper concentrations ranged from a low of ~5 nmol L^{-1} near the mouth to a maximum of ~60 nmol L^{-1} in the mid-south Bay. Concentrations were also high in the side basin samples within Shelter Island, where a large number of pleasure boats are moored.

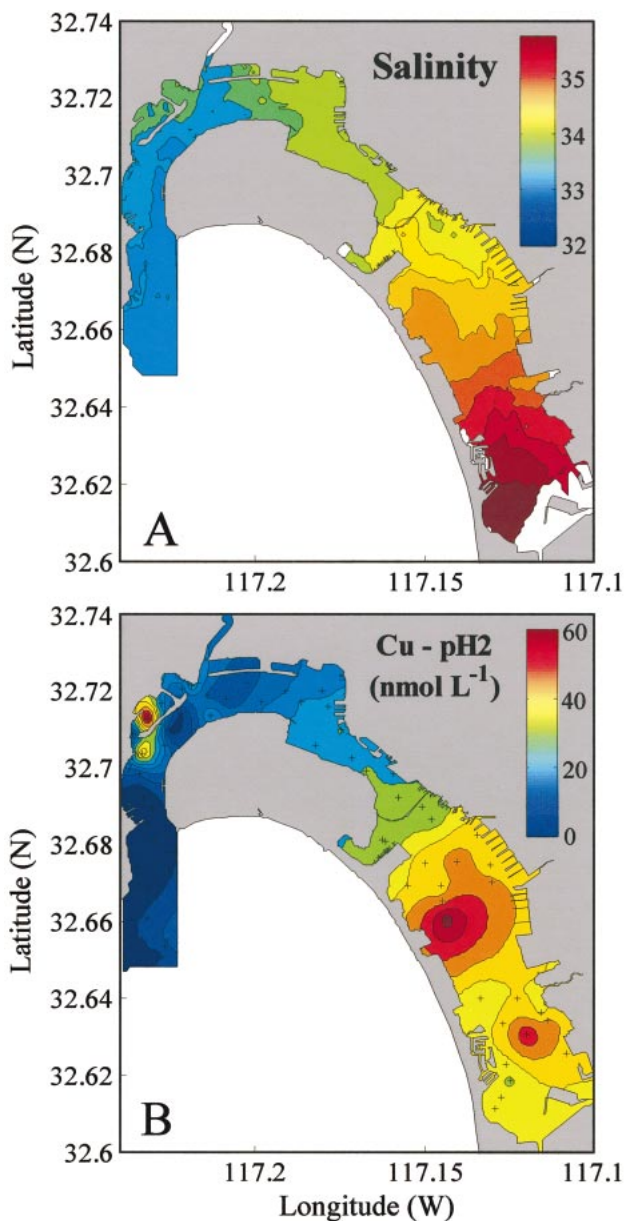


Fig. 3. The spatial distribution of (A) salinity and (B) copper measured by TMA at pH 2 in San Diego Bay for August 2000.

The distributions of dissolved copper, total copper, and TSS from the composite samples along the axis of the Bay are shown in Fig. 5. The four total copper distributions are remarkably similar and are consistent with the TMA mapping results, showing a general increase into the Bay from box 1 through box 20, followed by a slight decrease in the inner Bay (box 21 to box 25). Total copper concentrations ranged from a low of ~ 5 nmol L^{-1} to a maximum of nearly 60 nmol L^{-1} . The general pattern for dissolved copper was similar to the total, but with slightly lower concentrations. Fluctuations in copper concentrations among the four surveys were not large; highest levels for both total and dissolved copper were in January 2001, and lowest levels in most samples were in May 2001. The differences between

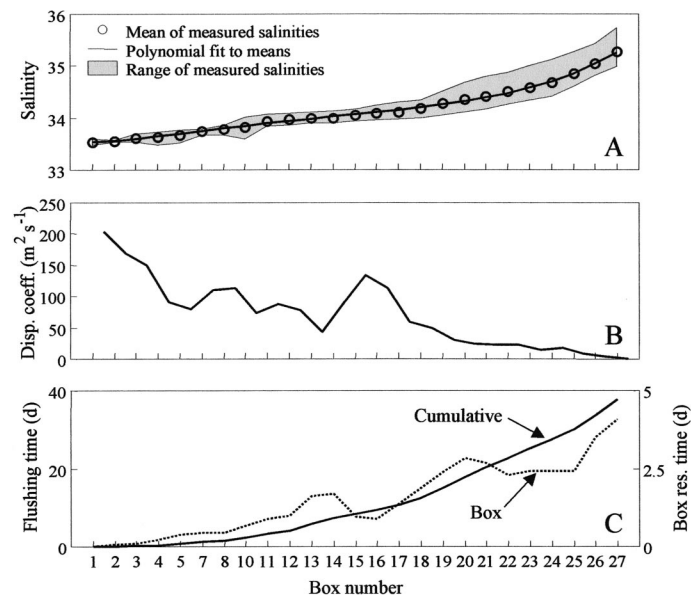


Fig. 4. The box-averaged longitudinal (A) salinity, (B) dispersion coefficient, and (C) residence time. In panel C, the solid black line corresponds to the left axis for flushing time, and the dotted black line corresponds to the right axis for individual box residence times.

surveys were small near the mouth but increased into the Bay to about 10 nmol L^{-1} .

The distribution of TSS showed similar patterns among the four surveys, with low levels near the mouth, increasing slightly in the outer Bay to about box 8, then decreasing somewhat into the mid-south Bay, and finally increasing

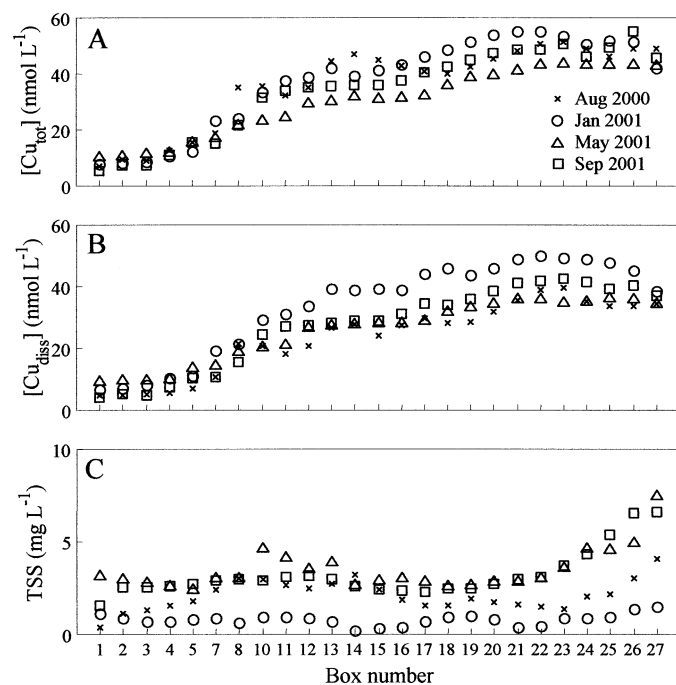


Fig. 5. Distribution of (A) total copper (Cu_{tot}), (B) dissolved copper (Cu_{dis}), and (C) TSS as a function of axial box number for the four surveys of San Diego Bay.

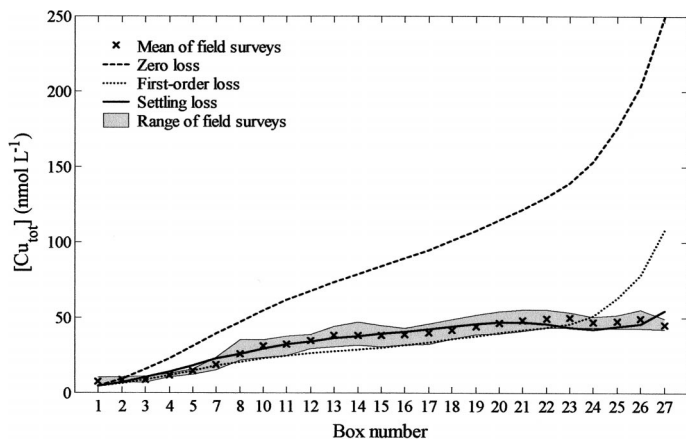


Fig. 6. Modeled and measured distribution of total copper (Cu_{tot}) in San Diego Bay, including the mean and range of measured copper concentrations for each box averaged across all surveys, the model result for conservative behavior (zero loss), the model result with a best-fit first-order loss rate of $7.4\% \text{ d}^{-1}$, and the model result for a best-fit uniform settling velocity of 1.4 m d^{-1} .

sharply near the head. In contrast to copper, for which the strongest spatial gradient was in the outer Bay, the strongest gradient for TSS was near the head. The overall range of TSS was from $<1 \text{ mg L}^{-1}$ to almost 8 mg L^{-1} . TSS levels during the January 2001 survey were substantially lower than all other surveys.

Modeling results—In our initial model runs for total copper, we assumed a conservative behavior for copper ($L = 0$) with no loss to the sediment. The results for this run (Fig. 6) give modeled water concentrations ranging from $\sim 10 \text{ nmol L}^{-1}$ at the mouth to $\sim 250 \text{ nmol L}^{-1}$ at the head; these are about five times higher than actual concentrations. Thus, in order to achieve a reasonable mass balance, a substantial fraction of the copper must be transported to the sediment.

In the following model runs, we adjusted the loss to the sediments assuming a first-order removal rate in relation to the water concentration (Eq. 7). A removal rate ranging from 6% to 9% d^{-1} gave concentrations that encompassed all measurements, and a best fit to the complete set of field data (not attempting to model individual surveys) was achieved with a loss rate of about $7.4\% \text{ d}^{-1}$ (Fig. 6). Although the fit of the modeled concentrations to the measured values is not ideal, this result does provide an idea of the general turnover time (half-life) for copper in the water column (4–7 d). With this first-order loss approach, the model tends to underestimate concentrations in the mid-Bay and overestimate concentrations near the head of the Bay. These discrepancies might be caused by the inability of a simple, first-order removal term to account for spatially varying factors such as water depth, particulate concentration, and settling characteristics.

In an attempt to account for some of these controlling factors and to improve the model results, we adopted the settling loss term described in Eq. 8. This loss term accommodates spatial variations in TSS and water depth and focuses on the settling of the particulate fraction as the primary exchange process with the sediment. In this case, an initial

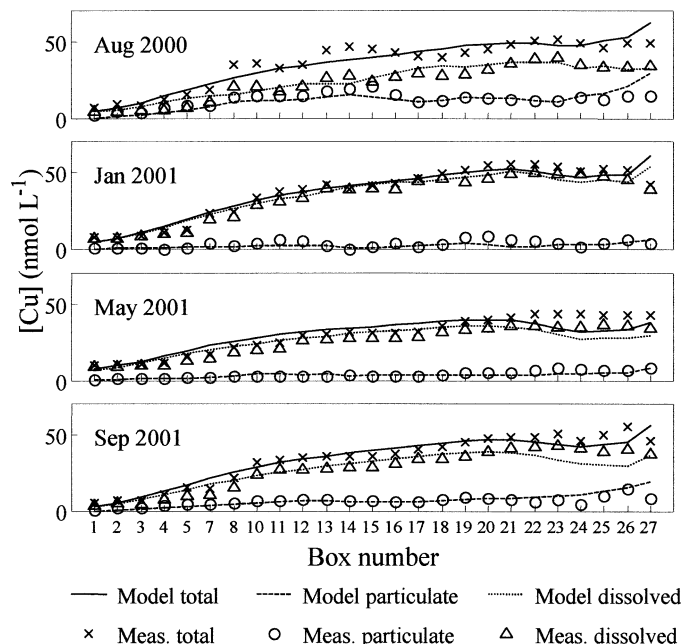


Fig. 7. Axial distribution of modeled and measured total, dissolved, and particulate copper in San Diego Bay. Model results for each survey are based on the best-fit partitioning coefficients and settling velocities shown in Table 3.

value of the partitioning coefficient was calculated from the field data by Eq. 9 and with the use of both the partitioning coefficient and the settling velocity as the fitting parameters, which were adjusted until the best fit was achieved with the field data for the total, dissolved, and particulate copper fractions. We first evaluated the best fit to the entire data set, neglecting temporal variations among the four surveys (Fig. 6). For the overall data set, we found $K_d = 0.1 \text{ L mg}^{-1}$, and $w = 1.4 \text{ m d}^{-1}$ gave a better fit to the general spatial trend in total copper when compared with the first-order removal approach (Fig. 6).

We then extended this approach to simulations for each individual survey period to evaluate the potential temporal variation in partitioning coefficients and settling rates suggested by the field data. In this case, individual partitioning coefficients and settling rates were determined for each survey, and the resulting dissolved, particulate, and total copper concentrations throughout the Bay were simulated (Fig. 7). Partitioning coefficients ranged from a low of 0.05 L mg^{-1} during the May 2001 survey to a high of 0.22 L mg^{-1} during the August 2000 survey, whereas settling velocities ranged from a low of 0.85 m d^{-1} for August 2000 to a high of 4.8

Table 3. Summary of best-fit modeling parameters for individual and combined survey conditions.

	Com- bined	Aug 2000	Jan 2001	May 2001	Sep 2001
c_i ocean (nmol L^{-1})	4.7	4.7	4.7	9.4	3.1
K_d (L mg^{-1})	0.1	0.22	0.06	0.05	0.08
w (m d^{-1})	1.4	0.85	4.8	3.3	1.3

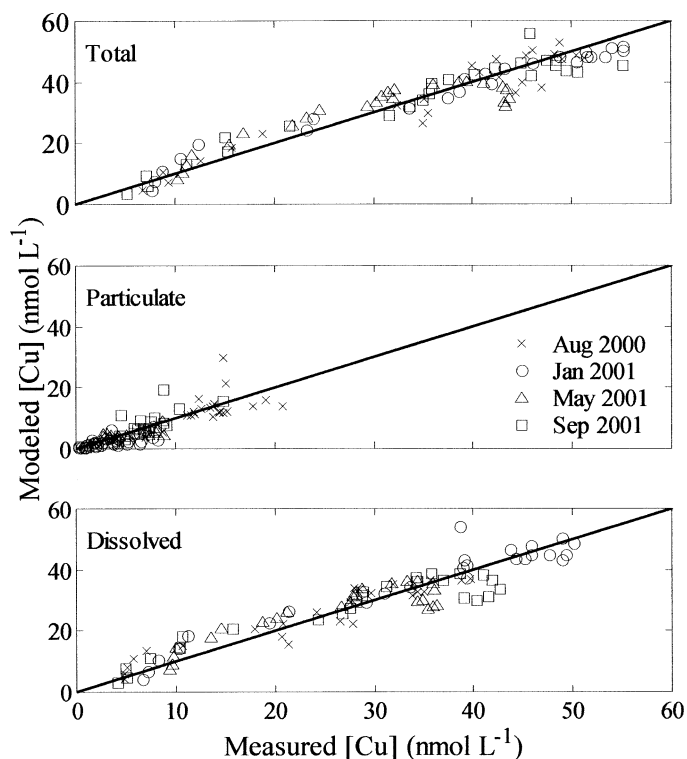


Fig. 8. Comparison of modeled and measured copper fractions for the surveys of August 2000, January 2001, May 2001, and September 2001. Solid lines represent a one-to-one relationship.

m d^{-1} for January 2001 (Table 3). The resulting comparisons between the field data and the model predictions are quite good, with 91%, 73%, and 88% of the variance in the field data for total, particulate, and dissolved copper, respectively, explained by the model (Fig. 8).

Discussion

The spatial distribution of total copper in the Bay is remarkably consistent over the four surveys. This finding supports the conceptual view that the mass balance of copper in the Bay is dominated by chronic sources and that this balance probably approaches steady state. This view is also supported by previous studies over the last 25 yr that have found similar levels of copper in San Diego Bay (Zirino et al. 1978; Flegal and Sañudo-Wilhelmy 1993; Esser and Volpe 2002). The highest concentrations of total copper were observed during January 2001, which is consistent with an increased loading from stormwater sources. The longitudinal pattern of the total copper distributions reflects the balance of flushing, sources, and losses. For example, consistently low concentrations of copper in the outer Bay reflect the strong ocean flushing and lack of sources in this region. The consistent peak between box 8 and box 12 (Fig. 5) coincides with the significant concentration of sources in this area (primarily pleasure boats), whereas the peak centered near box 18 coincides with a second group of sources in this area (primarily Navy ships).

The model results indicate the importance of nonconser-

vative processes (with respect to the water column) in controlling the mass balance of copper. The total copper concentration distribution predicted on the basis of the balance of sources and mixing alone substantially overestimates the measured concentrations in the Bay. Applying a simple, first-order loss term brings the predictions more in line with the measurements but fails to capture either the character of the distribution or the processes that control it. For San Diego Bay, it is clear that transport of waterborne copper to the sediment is also important. By integrating a settling loss term into the total copper model, the copper budget is balanced in a way that provides good agreement with the spatial distribution of copper in the Bay water.

The modeling analysis indicates a dissolved-particulate copper partitioning coefficient ranging from 0.05 to 0.22 L mg^{-1} , with a value of 0.1 L mg^{-1} for the survey-mean condition. The range of partitioning coefficients observed in this study is consistent with the range of values from similar coastal systems, including the southern coast of England (0.003–0.12; Comber et al. 2002), Melbourne Harbor, Australia (0.07; Holbrook 1984), San Francisco Bay, California (0.07; Wood et al. 1995), and Galveston Bay, Texas (0.03; Wen et al. 1999). Of the four surveys, three are quite consistent (January 2001, May 2001, September 2001), whereas the partitioning coefficient for the August 2000 survey is somewhat larger, indicating a preferential partitioning to the particulate phase.

The model results also provide estimated settling velocities. Because settling is the only sediment–water exchange process considered in the model, these velocities must be viewed as “effective” in the sense that they describe a net process that incorporates settling as well as additional processes such as sediment resuspension and benthic fluxes. The range of these effective settling velocities (0.85–4.8 m d^{-1}) and partitioning coefficients provide some insight into the possible characteristics of the particulate material that control the transport of copper to the sediment. For example, the results for August 2000 indicate particulate material with a strong affinity for copper but a relatively low effective settling velocity. In contrast, the results from May 2001 indicate particulate matter with a weaker affinity for copper, and a significantly faster (about four times) settling velocity. On the basis of these differences, one explanation could be that the particulate matter for the May 2001 survey was composed of a coarser, less reactive inorganic material. Some indirect support for this is provided by the comparatively high concentrations of DOC present during the August 2000 survey ($180 \mu\text{mol L}^{-1}$) compared to the May 2001 survey ($140 \mu\text{mol L}^{-1}$). Shifts in pH might also lead to changes in partitioning (Balistrieri and Murray 1983); however, the observed range of pH over the surveys, ~ 7.9 – 8.2 , is relatively narrow.

An alternative hypothesis is that although the settling rates vary, the partitioning between the particulate and the dissolved phase is kinetically controlled. In this case, we would expect that for faster settling rates we would observe smaller partitioning coefficients because the particulate material settles through the water column faster than the dissolved and particulate copper phases can equilibrate (Nyffeler et al. 1984; Wood et al. 1995). To illustrate this mechanism, we

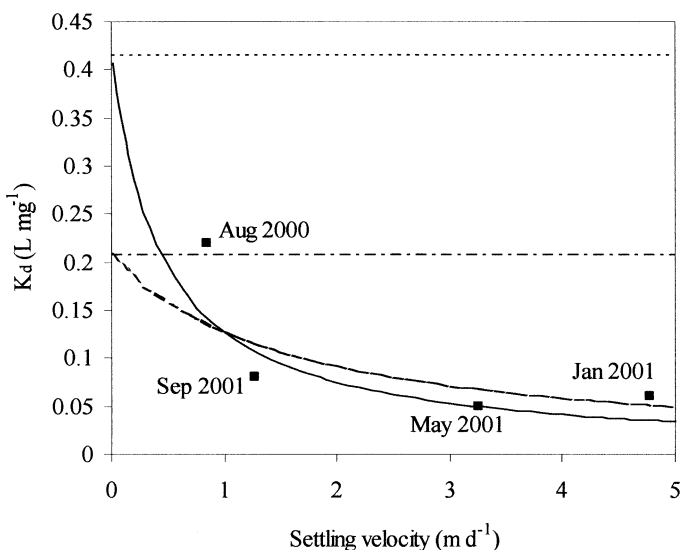


Fig. 9. The relationship between partitioning coefficient (K_d) and settling velocity (w). Solid squares are based on model parameters for the four survey conditions (see Table 3). The solid and dashed lines are the calculated relationship from Eq. 12 using $k_b = 0.12$ and $0.43 \text{ L mg}^{-1} \text{ d}^{-1}$, respectively (from Gee and Bruland 2002); $h = 3.6 \text{ m}$; and best-fit values of k_f . The dotted and dash-dot lines represent the expected equilibrium values of K_d for $w = 0$.

consider a simple scenario in which the concentration of particulate copper is controlled by a steady-state balance between kinetic partitioning from the dissolved phase and settling (neglecting tidal mixing) such that

$$V \frac{dc_p}{dt} = V k_f c_d \text{TSS} - V k_b c_p - \frac{w}{h} V c_p = 0 \quad (11)$$

where k_f is the forward rate constant, k_b is the backward rate constant, and other variables are as previously defined. By rearranging terms, we can recreate the form of Eq. 9 that defines the partitioning coefficient as

$$K_d = \frac{c_p}{c_d \text{TSS}} = \frac{k_f}{k_b + \frac{w}{h}} \quad (12)$$

from which it is apparent that the partitioning coefficient departs from the conventional definition $K_d = k_f/k_b$ when w/h is of order k_b .

The model results, together with recent estimates of kinetic rate constants (Gee and Bruland 2002) can be used to evaluate the general sense of this relationship. The results of Gee and Bruland (2002) for San Francisco Bay waters indicate average k_b values ranging from about 0.12 to 0.43 d^{-1} . Given the mean settling depth (half-water column depth) for San Diego Bay of about 3.6 m, the estimated range of w/h is 0.23–1.3 d^{-1} , suggesting that settling might be of greater importance than desorption within the balance of Eq. 12. Applying these k_b values to Eq. 12, we also estimated the range of k_f by fitting Eq. 12 to the available data for K_d and w from San Diego Bay (Fig. 9). Best-fit estimates suggest k_f ranging from ~ 0.05 to $0.09 \text{ L mg}^{-1} \text{ d}^{-1}$. Given the survey-

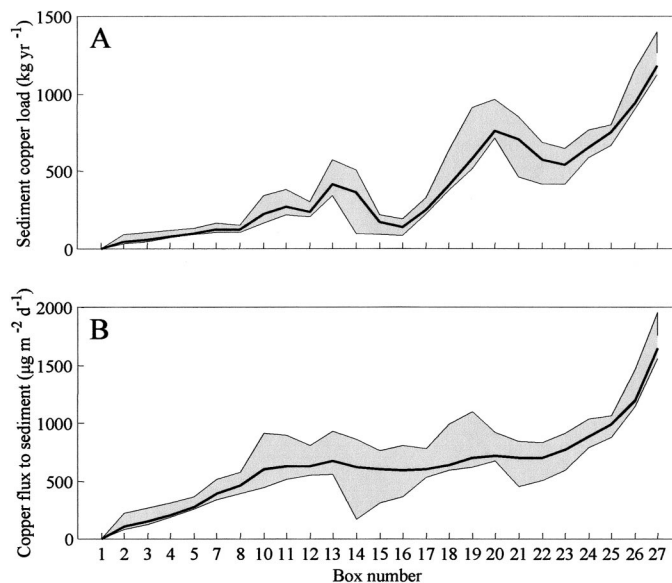


Fig. 10. Model estimates of (A) total copper load to sediment and (B) area-normalized total copper load. Solid line is based on the survey-average condition, and the shaded region represents the range of variation among the four surveys.

average TSS concentration in San Diego Bay of about 2.55 mg L^{-1} , this would correspond to a first-order forward rate constant ($k'_f = k_f \text{TSS}$) ranging from 0.13 to 0.23 d^{-1} , which is consistent with the range reported by Gee and Bruland (2002) of 0.07–0.20 d^{-1} for San Francisco Bay. Together, these results support the hypothesis that variations in observed partitioning coefficients could result from a balance between the forward reaction rate and the effective settling rate, as opposed to an equilibrium resulting from the balance of the forward and backward reaction rates. In addition, the findings suggest that a copper fate model that incorporated kinetic rates rather than equilibrium conditions could explain some of the variations observed among surveys in San Diego Bay.

The settling loss term from the model provides a direct estimate of the loading of copper to the sediment. These loadings were evaluated for both the survey-mean condition and the individual surveys. On the basis of the estimate for the survey-mean condition, the sediment loading ranges from 45 to 1,180 kg yr^{-1} , with the highest loading predominantly to the inner Bay, even though the sources are distributed in both the inner and outer Bay (Fig. 10). This appears to result from several factors, including the elevated particulate copper levels, shallow water, and long residence times that are all characteristic of the inner Bay. Integration of the sediment load throughout the Bay indicates a total loss of $\sim 9,700 \text{ kg yr}^{-1}$ to the sediments of San Diego Bay. Of the 9,700 kg yr^{-1} that enters the sediment, 83% is to the inner Bay (boxes 14–25), and only 17% is to the outer Bay (boxes 2–13). In contrast, only 57% of the loading is to the inner Bay, whereas 43% is to the outer Bay. Given the total annual loading of copper to the Bay of about $20.4 \times 10^3 \text{ kg yr}^{-1}$, this balance suggests that about 48% of the input is

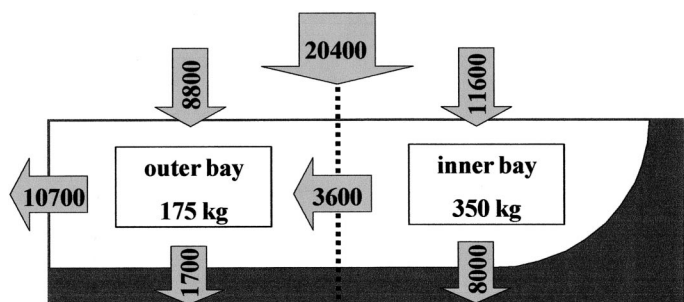


Fig. 11. Estimated dry-weather mass balance for total copper in San Diego Bay. All fluxes are in units of kg yr^{-1} . Boxes represent the estimated steady-state reservoirs for total copper in the water column of the outer and inner Bay regions.

transported to the sediment, and the remaining 52% is flushed to the ocean (Fig. 11).

The relative importance of benthic fluxes in this balance can be assessed by comparing the loss terms attributable to the effective settling velocities and measured benthic flux rates. Measurements of benthic fluxes in San Diego Bay indicate copper fluxes ranging from about $-100 \mu\text{g m}^{-2} \text{d}^{-1}$ to $300 \mu\text{g m}^{-2} \text{d}^{-1}$ (Chadwick et al. 1999), which is consistent with the range reported in other urbanized coastal harbors (Kuwabara et al. 1996; Rivera-Duarte and Flegal 1997). Normalizing the loss rates from the model to the surface area for each box gives rates ranging from 104 to $1,644 \mu\text{g m}^{-2} \text{d}^{-1}$, with the majority of the Bay $>500 \mu\text{g m}^{-2} \text{d}^{-1}$ (Fig. 10). These results indicate that benthic fluxes might play some role in exchange of copper between the water column and sediment but that the primary pathway is probably particle settling. This is in contrast, for example, to the findings of Wood et al. (1995) and Rivera-Duarte and Flegal (1997), in which both diagnostic modeling and direct measurement suggested that benthic fluxes were probably a dominant source of copper to South San Francisco Bay.

The loading diagrams shown in Fig. 11 suggest that accumulation of copper in the sediments of San Diego Bay should increase substantially from the outer Bay to the inner Bay. To verify this result, we compiled solid-phase sediment copper data from historical studies in San Diego Bay (Fairey et al. 1998; Chadwick et al. 1999; Noblet et al. 2002). These data were filtered to remove stations within side basins and pier areas, binned by location to the nearest model box, then averaged (Fig. 12). Note that insufficient data were available to determine a solid-phase sediment copper concentration for box segments 1, 2, and 27. The distribution of copper in the sediments of San Diego Bay appears to reflect the modeled loading, although the sediment concentrations near the head of the Bay are somewhat lower than might be expected from the loading diagram (Fig. 10).

A rigorous, system-wide field program has been integrated with a one-dimensional modeling system to evaluate the overall mass balance of copper in a representative coastal harbor. The field investigations employed a combination of novel and traditional analytical tools to determine the Bay-wide distribution of total copper and important fractions of the copper pool. The spatial distribution of copper in the Bay reflects the balance of sources, flushing, and losses to

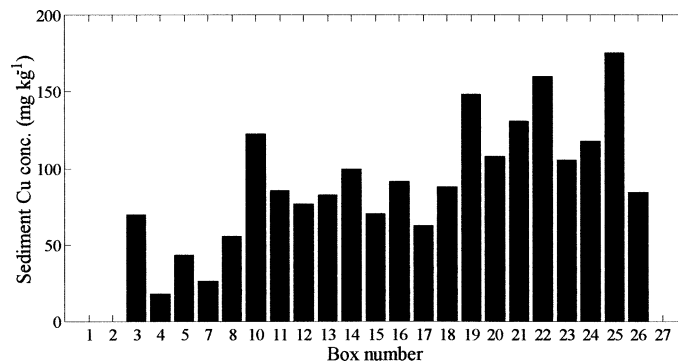


Fig. 12. Box-averaged distribution of copper concentration in the sediments of San Diego Bay.

the sediment. Variations in the distribution of total copper from survey to survey appear to be small, with the largest difference observed during the winter, corresponding with elevated sources associated with stormwater flows. Modeling results illustrate the importance of losses of copper to the sediment. Without this loss term in the model, water column concentrations are overestimated by as much as a factor of five. The time scale for the loss term appears to be on the order of 8–10 d, and the model reproduced the field measurements quite well with the use of a loss term controlled by partitioning and settling parameters. The variation of these parameters from survey to survey indicates the possibility that the partitioning is controlled by a balance between the forward reaction rate and the settling rate, as opposed to an equilibrium condition. The overall balance of total copper in the Bay appears to be split between losses to the ocean via tidal flushing and losses to the sediments via settling. Thus, it is clear that settling plays a key role in the fate of copper in the Bay and that the sediments are a key endpoint for copper fate. This finding is substantiated by historical data for the spatial distribution of sediment copper levels in San Diego Bay.

References

- BALISTRERI, L. S., AND J. W. MURRAY. 1983. Metal–solid interactions in the marine environment: Estimating apparent equilibrium binding constants. *Geochim. Cosmochim. Acta* **47**: 1091–1098.
- BRULAND, K. W., K. H. COALE, AND L. MART. 1985. Analysis of seawater for dissolved cadmium, copper and lead—an inter-comparison of voltammetric and atomic-absorption methods. *Mar. Chem.* **17**: 285–300.
- CANTWELL, M. G., R. M. BURGESS, AND D. R. KESTER. 2002. Release and phase partitioning of metals from anoxic estuarine sediments during periods of simulated resuspension. *Environ. Sci. Technol.* **36**: 5328–5334.
- CHADWICK, D. B., AND J. L. LARGIER. 2000. Tidal exchange at the bay–ocean boundary. *J. Geophys. Res.* **104**: 29,901–29,924.
- , AND OTHERS. 1999. Sediment quality characterization—Naval Station San Diego. Space and Naval Warfare Systems Center San Diego Technical Report 1777.
- COMBER, S. D. W., G. FRANKLIN, M. J. GARDNER, C. D. WATTS, A. B. A. BOXALL, AND J. HOWCROFT. 2002. Partitioning of marine antifoulants in the marine environment. *Sci. Total Environ.* **286**: 61–71.

- DI TORO, D. M., H. E. ALLEN, H. L. BERGMAN, J. S. MEYER, P. R. PAQUIN, AND R. C. SANTORE. 2001. Biotic ligand model of the acute toxicity of metals, 1. Technical basis. *Environ. Toxicol. Chem.* **20**: 2383–2396.
- DYER, K. R. 1974. The salt balance in stratified estuaries. *Estuar. Coast. Mar. Sci.* **2**: 275–281.
- ERIKSEN, R. S., D. J. MACKAY, R. VAN DAM, AND B. NOWAK. 2001. Copper speciation and toxicity in Macquarie Harbour, Tasmania: An investigation using a copper ion selective electrode. *Mar. Chem.* **74**: 99–113.
- ESSER, B. K., AND A. VOLPE. 2002. At-sea high-resolution trace element mapping: San Diego Bay and its plume in the adjacent coastal ocean. *Environ. Sci. Technol.* **36**: 2826–2832.
- FAIREY, R., AND OTHERS. 1998. An assessment of sediment toxicity and chemical concentrations in the San Diego Bay region. *Environ. Toxicol. Chem.* **17**: 1570–1581.
- FISCHER, H. B., E. J. LIST, R. C. Y. KOH, J. IMBERGER, AND N. H. BROOKS. 1979. Mixing in inland and coastal waters. Academic Press.
- FLEGAL, A. R., AND S. SAÑUDO-WILHELMY. 1993. Comparable levels of trace metal contamination in two semi-enclosed embayments: San Diego Bay and South San Francisco Bay. *Environ. Sci. Technol.* **27**: 1934–1936.
- GEE, A. K., AND K. W. BRULAND. 2002. Tracing Ni, Cu, and Zn kinetics and equilibrium partitioning between dissolved and particulate phases in South San Francisco Bay, California, using stable isotopes and high-resolution inductively coupled plasma mass spectrometry. *Geochim. Cosmochim. Acta* **66**: 3063–3083.
- HOLBROOK, S. H. 1984. Partitioning and fate of antifouling paint copper released into an estuarine environment. M.S. thesis, Florida Institute of Technology, Melbourne, Florida.
- JOHNSON, H. D., J. G. GROVHOUG, AND A. O. VALKIRS. 1998. Copper loading to U.S. Navy harbors. Space and Naval Warfare Systems Center San Diego Technical Document 3052.
- KATZ, C. N. 1998. Seawater polynuclear aromatic hydrocarbons and copper in San Diego Bay. Space and Naval Warfare Systems Center San Diego Technical Document 1768.
- KLINKHAMMER, G. P., AND M. L. BENDER. 1981. Trace metal distributions in the Hudson River Estuary. *Estuar. Coast. Shelf Sci.* **12**: 629–643.
- KUWABARA, J. S., C. C. Y. CHANG, A. I. KHECHFE, AND Y. R. HYNTER. 1996. Importance of dissolved sulfides and organic substances in controlling the speciation of heavy metals in San Francisco Bay, p. 157–172. *In* J. T. Hollibaugh [ed.], *San Francisco Bay: The ecosystem*. Pacific Division of the Association for the Advancement of Science.
- LARGIER, J. L., C. J. HEARN, AND D. B. CHADWICK. 1996. Density structures in low inflow estuaries, p. 155–174. *In* D. G. Aubrey and C. T. Friedrichs [eds.], *Buoyancy effects on coastal dynamics*. American Geophysical Union.
- , J. T. HOLLIBAUGH, AND S. V. SMITH. 1997. Seasonally hypersaline estuaries in Mediterranean-climate regions. *Estuar. Coast. Shelf Sci.* **45**: 789–797.
- MOFFETT, J. W., L. E. BRAND, P. L. CROOT, AND K. A. BARBEAU. 1997. Cu speciation and cyanobacterial distribution in harbors subject to anthropogenic Cu inputs. *Limnol. Oceanogr.* **42**: 789–799.
- NOBLET, J. A., E. Y. ZENG, R. BAIRD, R. W. GOSSETT, R. J. OZRETTICH, AND C. R. PHILLIPS. 2002. Southern California Bight 1998 Regional Monitoring Program: VI. Sediment chemistry. Southern California Coastal Water Research Project.
- NRIAGU, J. O. 1996. A history of global metal pollution. *Science* **272**: 223–224.
- NYFFELER, U. P., Y.-H. LI, AND P. H. SANTSCHI. 1984. A kinetic approach to describe trace-element distribution between particles and solution in natural aquatic systems. *Geochim. Cosmochim. Acta* **48**: 1513–1522.
- QIAN, J. G., AND K. MOPPER. 1996. Automated high performance, high-temperature combustion total organic carbon analyzer. *Anal. Chem.* **68**: 3090–3097.
- RANKE, J. 2002. Persistence of antifouling agents in the marine biosphere. *Environ. Sci. Technol.* **36**: 1539–1545.
- RIVERA-DUARTE, I., AND A. R. FLEGAL. 1997. Porewater gradients and diffusive benthic fluxes of Co, Ni, Cu, Zn, and Cd in San Francisco Bay. *Croat. Chem. Acta* **70**: 389–417.
- ROZAN, T. F., AND G. BENOIT. 2001. Mass balance of heavy metals in New Haven Harbor, Connecticut: Predominance of nonpoint sources. *Limnol. Oceanogr.* **46**: 2032–2049.
- SANTSCHI, P. H., S. NIXON, M. PILSON, AND C. HUNT. 1984. Accumulation of sediments, trace metals (Cu, Pb) and total hydrocarbons in Narragansett Bay, Rhode Island. *Estuar. Coast. Shelf Sci.* **19**: 427–429.
- SPINELLI, G. A., A. T. FISHER, C. G. WHEAT, M. D. TRYON, K. M. BROWN, AND A. R. FLEGAL. 2002. Groundwater seepage into northern San Francisco Bay: Implications for dissolved metals budgets. *Wat. Resour. Res.* **38**(12): 1–19.
- TERLIZZI, A., S. FRASCHETTI, P. GIANGUZZA, M. FAIMALI, AND F. BOERO. 2001. Environmental impact of antifouling technologies: State of the art and perspectives. *Aquat. Conserv.* **11**: 311–317.
- TIPPING, E. 1994. WHAM—A computer equilibrium model and computer code for waters, sediments, and soils incorporating a discrete site/electrostatic model of ion-binding by humic substances. *Comput. Geosci.* **20**: 973–1023.
- [USEPA] U.S. ENVIRONMENTAL PROTECTION AGENCY. 1999. Phase I uniform national discharge standards for vessels of the armed forces, technical development document. EPA 821-R-99-001.
- VALKIRS, A. O., P. F. SELIGMAN, E. HASLBECK, AND J. S. CASO. 2003. Measurement of copper release rates from antifouling paint under laboratory and in situ conditions: Implications for loading estimation to marine water bodies. *Mar. Pollut. Bull.* **46**: 763–779.
- WANG, P. F., R. T. CHENG, K. RICHTER, E. S. GROSS, D. SUTTON, AND J. W. GARTNER. 1998. Modeling tidal hydrodynamics of San Diego Bay, California. *J. Am. Water Res. Assoc.* **34**: 1123–1140.
- WEN, L. S., P. SANTSCHI, G. GILL, AND C. PATERNOSTRO. 1999. Estuarine trace metal distributions in Galveston Bay: Importance of colloidal forms in the speciation of the dissolved phase. *Mar. Chem.* **63**: 185–212.
- WOOD, T. M., A. M. BAPTISTA, J. S. KUWABARA, AND A. R. FLEGAL. 1995. Diagnostic modeling of trace metal partitioning in South San Francisco Bay. *Limnol. Oceanogr.* **40**: 345–358.
- ZIRINO, A., S. LIEBERMAN, AND C. CLAVELL. 1978. Measurement of Cu and Zn in San Diego Bay by automated anodic stripping voltammetry. *Environ. Sci. Technol.* **12**: 73–79.
- , S. L. BELLI, AND D. A. VANDERWEELE. 1998a. Copper concentration and Cu(II) activity in San Diego Bay. *Electroanalysis* **10**: 423–427.
- , D. A. VANDERWEELE, S. L. BELLI, R. DEMARCO, AND D. J. MACKAY. 1998b. Direct measurement of Cu(II)aq in seawater at pH 8 with the jalpaite ion-selective electrode. *Mar. Chem.* **61**: 173–184.

Received: 5 February 2003

Accepted: 1 September 2003

Amended: 4 November 2003